Time-resolved FTIR emission spectroscopy of Cu in the 18003800 cm1 region: transitions involving f and g states and oscillator strengths

S Civiš, I Matulková, J Cihelka, P Kubelk, K Kawaguchi, V E Chernov

Time-resolved FTIR emission spectroscopy of Cu in the 1800–3800 cm^{-1} region: Transitions involving f and g states and oscillator strengths

S Civiš[1], I Matulková[1], J Cihelka[1], P Kubelík[1], K Kawaguchi[2] and V E Chernov[3]

[1] J. Heyrovský Institute of Physical Chemistry, Academy of Sciences of the Czech Republic, Dolejškova 3, 18223 Prague 8, Czech Republic

E-mail: civis@jh-inst.cas.cz

[2] Faculty of Science, Okayama University, Tsushima-naka, Okayama 700-8530, Japan

[3] Voronezh State University, 394693 Voronezh, Russia

Abstract. Time-resolved Fourier-transform spectroscopy was applied to the study of the emission spectra of Cu vapors in a vacuum (10^{-2} Torr) produced in ablation of a Cu metal target by a high-repetition rate (1.0 kHz) pulsed nanosecond ArF laser ($\lambda = 193$ nm, output energy of 15 mJ). The time-resolved infrared emission spectrum of Cu was recorded in the 1800–3800 cm^{-1} spectral region with a resolution of 0.017 cm^{-1}. The time profiles of the measured lines have maxima at 18–20 μs after a laser shot and display non-exponential decay with a decay time of 5–15 μs. This study reports 17 lines (uncertainty 0.0003–0.018 cm^{-1}) of Cu I not previously observed. This results in 7 newly-found levels and revised energy values for 11 known levels (uncertainty 0.01–0.03 cm^{-1}). We also calculate transition probabilities and oscillator strengths for several transitions involving the reported Cu levels.

PACS numbers: 52.38.Mf, 07.57.Ty, 32.30.Bv, 31.15.B-

Submitted to: *J. Phys. B: At. Mol. Phys.*

Keywords:Time-resolved Fourier transform infrared spectroscopy, time decay of spectral lines, Atomic ablation, Cu, Copper, Rydberg states, oscillator strengths, line strengths, dipole transition matrix elements

1. Introduction

The great advantages of Fourier transform infrared spectroscopy (FTIR), such as its constant high resolution and energy throughput, have made the IR spectral region more accessible for laboratory spectral measurements (Nilsson, 2009). The infrared range is becoming more and more important in astronomical research, for instance in studies of dust-obscured objects and interstellar clouds, cool objects such as discs, planets and the extended atmospheres of evolved stars, including objects at cosmological distances from the Earth (Kerber et al., 2009). Nevertheless, the powerful capacities of IR astronomy (*e. g.* ESOs CRyogenic Infra-Red Echelle Spectrograph, CRIRES) cannot be fully utilized without detailed spectroscopical information, first of all, on atomic line wavelengths and oscillator strengths in the IR region (Biémont, 1994; Grevesse and Noels, 1994; Pickering, 1999; Jorissen, 2004; Johansson, 2005). A general drawback of the IR spectral region is the much lower number of atomic and ionic lines available (as compared to the visible and ultraviolet range) (Ryde, 2010), so reporting new IR atomic lines is important.

Cu is the element (together with Zn) immediately following the iron peak, and its abundance is important in studies of scenarios of the chemical evolution of the Galaxy implied by different nucleosynthesis models (Sneden et al., 1991; Matteucci et al., 1993; Prochaska et al., 2000; Cunha et al., 2002; Mishenina et al., 2002; Simmerer et al., 2003; Bihain et al., 2004; Ecuvillon et al., 2004; Sobeck et al., 2008). Copper abundance can be analyzed from the IR spectra of cool stars (Ryde, 2009; Wahlgren et al., 2009), metal-poor stars (Cowan et al., 2002; Honda et al., 2007) and substellar objects (Jones et al., 2005).

It should be noted that the studies of copper abundances in stars and the interstellar medium were performed mostly with optical 510.554 nm, 521.820 nm and 578.212 nm (Sneden et al., 1991; Mishenina et al., 2002; Cunha et al., 2002; Simmerer et al., 2003; Ecuvillon et al., 2004; Prochaska et al., 2000) or ultraviolet 327.395 nm (Bihain et al., 2004; Sobeck et al., 2008) and 324.754 nm (Sobeck et al., 2008) Cu I lines. To our knowledge, no infrared lines of Cu I were involved in the abundance analysis except the 809.263 nm line used in a study of stellar abundances in the thick disc of the Galaxy (Prochaska et al., 2000). Nor have we encountered literature data about Cu I lines with wavelengths above 2 microns, and the present work is intended to supply information about Cu I infrared lines and transition moments in the 2.7–5.5 micron range. This work continues the previous studies on Au I (Civiš et al., 2010) and Ag I (Civiš et al., 2010).

Atomic copper has been attracting the great interest of spectroscopists for many decades, since its spectrum gives one of the best examples of the majority of peculiarities in atomic spectra due to a number of series perturbations observed below the first ionization threshold. Analysis of the main features of the Cu I spectrum began in the 1920s, and the first critical and exhaustive study of Cu I lines and levels was reported by Shenstone (1948). He published the spectrum from 150.4 nm to 1822.9 nm (5484–

66485 cm^{-1}) including both his own measurements and the previous results of other authors.

The simplest Cu I term structure originates from the closed $3d^{10}$ core yielding $3d^{10}\,nl_j$ states with a total angular momentum $J = j = l \pm \frac{1}{2}$. Other terms arise due to excitation of a 3d electron into a $n'l'$ state. The core-excited $3d^9\,nln'l'$ Cu I states were studied both by numerical *ab initio* calculations (Martin and Sugar, 1969; Carlsson, 1988) and by VUV photoabsorption (Tondello, 1973; Longmire et al., 1980; Baig et al., 1992); for a more detailed review see (Baig et al., 1997). The most comprehensive reports of the closed-core $3d^{10}\,nl_j$ states of Cu were made by Longmire et al. (1980) (for ns states up to $n = 41$ and np states up to $n = 57$) and by MacAdam et al. (2009) (for s, p, d, f and g states for $n = 23$–28).

The aim of the present work is the study of the Cu I spectrum in the infrared domain using FTIR spectroscopy of laser-ablated Cu plasma. The lines in this domain are due to transitions between the levels with $n = 4$–7; the energies of some levels (for f and g states) have not been previously reported. To identify the transitions involving these and other low-Rydberg Cu levels, we use the information on the relative intensity of the transitions obtained here by the calculation of dipole transition matrix elements (or transition dipole moments) using the Fues model potential (FMP) approach (Civiš et al., 2010). The comparison tables presented in Section 3.1 show a reasonable agreement between our calculations and the experimental and theoretical results for oscillator strengths. The dipole transition matrix elements calculated in the Section 3.1 are used in Sec. 3.2 for classification of the observed lines resulting in revised values for some terms of Cu I.

2. Method

The experimental setup has already been described in detail in our previous papers (Civiš et al., 2010; Kawaguchi et al., 2008). The time resolution FTIR spectra were measured using the modified Bruker IFS 120 HR spectrometer in J. Heyrovský Institute in Praha. The modification of the apparatus for the time-resolution scan of emission data was previously developed in Okayama University. The Bruker high resolution interferometer is calibrated against the internal stabilised HeNe laser with a precision around 0.001 cm^{-1}.

The Bruker system was equipped with an analog-digital converter (ADC 4322: Analogic, USA), which was connected to a PC containing a programmable control processor of Field Programmable Gate Array – FPGA, (ACEX 1K: Altera, USA) set up at a frequency of 33 MHz, and digital input board PCI (2172C: Interface, Japan). The data collection process and synchronization with the laser were controlled by the FPGA processor programmed by QUARTUS II 7.1, Altera. The software for data acquisition and fast FT transformation and displaying of the data were written in C $^{++}$ language.

Time-resolved FTIR spectroscopy was applied for observations of the emission arising after the irradiation of metals with a pulsed nanosecond ArF ($\lambda = 193$ nm) laser.

A high repetition rate ArF laser ExciStar S-Industrial V2.0 1000 (193 nm, laser pulse width 12 ns, frequency 1 kHz) with 15 mJ output power was focused on a rotating and linearly traversing copper target inside a vacuum chamber (average pressure 10^{-2} Torr). The infrared emission (axial distance from the target 10 mm) was focused into the spectrometer using a CaF_2 (100 mm) lens. The emission was observed in the 1800–3800 cm^{-1} spectral region with a time profile showing maximum emission intensity at 18–20 μs after the laser shot.

For data sampling we used the so-called 1/3 sampling, where the scanner rate was set to produce a 3 kHz HeNe laser interference signal, the ArF laser oscillation was triggered, and 60 sets of time-resolved data were recorded with a preset time interval of 1 μs. Three scans were needed for a complete interferogram, and only 5 scans were coadded to improve the signal-to-noise ratio (SNR). The spectral resolution in such a procedure was about 0.1 cm^{-1}. We also performed measurements with only one scan but with higher resolution of about 0.017 cm^{-1} but worse SNR. The acquired spectra were post-zerofilled (zero filling 2, trapezoid apodization function) using the Bruker OPUS sowtware and subsequently corrected by subtracting the blackbody background spectrum. The wavenumbers, line widths and their intensities were then obtained using the OPUS internal peak picking procedure.

The Fues model potential method for the calculation of dipole matrix elements was outlined in the previous paper (Civiš et al., 2010). For Cu I the radial quantum number n_r (which is equal to the number of nodes of the radial wavefunction) was assumed as:

$$n_r = \begin{cases} n-4 & \text{for s, p, d-states } (n \geq 4); \\ n-l-1 & \text{for } l \geq 3 \text{ states } (n \geq l+1). \end{cases} \quad (1)$$

3. Results and discussion

3.1. Calculation of the dipole transition matrix elements

It is generally considered that the choice of a Coulomb approximation monoconfigurational approach (such as the FMP approach used here) is justified for transitions involving high-energy unperturbed Rydberg states, these transitions appearing mostly in IR region considered here. This approach however is reasonable for calculation of transitions involving also low-excited and even ground states. The comparison of FMP calculations with experimental and theoretical results (including *ab initio* calculations) for transitions in Ag was presented in the previous paper (Civiš et al., 2010). It was shown that the agreement of FMP calculations with the experiment and with the results of other calculations is satisfactory for the majority of transitions. For few transitions there were some discrepancies. However, the results of other theoretical calculations for these transitions differ between each other by some orders of magnitude and some are close to our results. From the other hand, the FMP calculations themselves are not our main aim in the present work; we use them in analyzing the relative intensities of the observed IR transitions only. To show that FMP calculation of dipole transition matrix

elements are adequate for such a purpose we compare some FMP-calculated Cu oscillator strengths with the experimental and theoretical data available in the literature.

The results of such a comparison with the experiment and with other calculations are presented in Table 1. The overall agreement of our calculations with other results can be considered to be reasonable. There are some large discrepancies between our data and the values from the half-century old sources given by Allen and Asaad (1957) for 4p–ns transitions with $n = 7, 8, 9$. In such cases, Table 1 contains the corresponding oscillator strength values calculated in Coulomb-like approximation (Lindgård et al., 1980). We did not present here a full comparison with Lindgård et al. (1980) because of the large data reported in it. However, since the Coulomb-like approximation used by Lindgård et al. (1980) is in essence similar to FMP, the majority of the results of Lindgård et al. (1980) coincide with the FMP values with a discrepancy of not more than 20%. We demonstrate this in the Table 2 for the transitions involving the Cu I states observed in our experiment. All the uncertainties in the tables below are given in round brackets after the corresponding values and should be treated as their rightmost significant digits, *e. g.* 123.4(56) means 123.4 ± 5.6.

The further analysis of the observed Cu lines given in the next Section is based on FMP calculation of the line strengths S for transitions between the $3d^{10}\, nl_j$ states which can be easily obtained from oscillator strengths f or transition probabilities A presented in Table 2. When available, the corresponding results of (Lindgård et al., 1980) were presented for comparison; the other values have not been reported previously. The Table 2 can serve as a supplement to the tables of Lindgård et al. (1980) and to the review by Fu et al. (1995).

3.2. Lines observed

Figure 1 shows parts of the observed IR emission spectra of Cu I at 20 μs after the laser shot, when the emission intensity is maximal for almost all of the observed lines. The list of the IR lines observed for Cu I is presented in Table 3. Their full widths at half-maxima (FWHM) are calculated from fitting to the Lorentzian shape (Civiš et al., 2010; Civiš et al., 2010).

As in the previous papers (Civiš et al., 2010; Civiš et al., 2010) we have measured the emission spectrum at a different delay time, from 0 to 60 μs after the laser shot. This allows us to record the the time profiles of the observed Cu lines, *i. e.* their emission intensities $I(t)$ as functions of the delay time, t. Such information can be helpful for diagnostics of the electronic state populations of neutral atoms in plumes formed by pulsed laser ablation Furusawa et al. (2004); however there are few reports of investigations on such population dynamics Rossa et al. (2009). The temporal dynamics of several lines is shown in Figure 2. While the temporal decay of some lines can be fitted, at least roughly, by an exponential function

$$I(t) = I_{\text{background}} + I_0 \exp\left(-\frac{t - t_0}{T}\right), \tag{2}$$

Table 1. Comparison of FMP-calculated oscillator strengths for transitions between some $3d^{10}\,nl_j$ states of Cu I with the values from other sources

Transition	FMP (this work)	Other values
$4s_{\frac{1}{2}}$–$4p_{\frac{1}{2}}$	0.223	0.22175[a]; 0.215(6)[b]; 0.2631[c]; 0.214[d]; 0.224[e]; 0.215[f]; 0.220(15)[g]; 0.22[h]; 0.2230[j]; 0.323(4)[l]; 0.153[k]; 0.16(4)[m]; 0.0158[n]
$4s_{\frac{1}{2}}$–$4p_{\frac{3}{2}}$	0.449	0.44756[a]; 0.439(12)[b]; 0.5296[c]; 0.432[d]; 0.453[e]; 0.434[f]; 0.432(28)[g]; 0.43(2)[i]; 0.4460[j]; 0.66[l]; 0.322[k]; 0.31(3)[m]; 0.0316[n]
$4p_{\frac{1}{2}}$–$5s_{\frac{1}{2}}$	0.171	0.151[e]; 0.1690[j]
$4p_{\frac{3}{2}}$–$5s_{\frac{1}{2}}$	0.172	0.153[e]; 0.1730[j]
$4p_{\frac{1}{2}}$–$6s_{\frac{1}{2}}$	0.0134	0.0136[e]; 0.00909[j]; 0.0148[n]
$4p_{\frac{3}{2}}$–$6s_{\frac{1}{2}}$	0.0131	0.0136[e]; 0.0131[j]; 0.0157[n]
$4p_{\frac{3}{2}}$–$6d_{\frac{5}{2}}$	0.0465	0.04441[c]; 0.00378[n]
$4p_{\frac{1}{2}}$–$7s_{\frac{1}{2}}$	0.00419	0.004064[c]; 0.00723[n]
$4p_{\frac{1}{2}}$–$8s_{\frac{1}{2}}$	0.00191	0.001899[c]; 0.00245[n]
$4p_{\frac{1}{2}}$–$9s_{\frac{1}{2}}$	0.00105	0.001053[c]; 0.000251[n]
$4p_{\frac{3}{2}}$–$9s_{\frac{1}{2}}$	0.00102	0.001027[c]; 0.00056[n]
$4p_{\frac{1}{2}}$–$4d_{\frac{3}{2}}$	0.592	0.51106[a]; 0.551[d]; 0.546[e]; 0.4880[j]
$4p_{\frac{3}{2}}$–$4d_{\frac{5}{2}}$	0.538	0.46727[a]; 0.503[d]; 0.499[e]; 0.4650[j]
$4p_{\frac{3}{2}}$–$4d_{\frac{3}{2}}$	0.0598	0.05201[a]; 0.056[d]; 0.0555[e]; 0.0614[j]
$4p_{\frac{1}{2}}$–$5d_{\frac{3}{2}}$	0.131	0.1238[c]; 0.117[e]; 0.0932[j]
$4p_{\frac{3}{2}}$–$5d_{\frac{5}{2}}$	0.118	0.1114[c]; 0.107[e]; 0.0791[j]
$4p_{\frac{3}{2}}$–$5d_{\frac{3}{2}}$	0.0131	0.01236[c]; 0.0119[e]

[a] Solution of one-electron Schrödinger equation with Hartree–Slater potential corrected by core polarisation and spin-orbital interaction (Curtis and Theodosiou, 1989)
[b] Laser-induced fluorescence from sputtered metal vapors (Hannaford and Lowe, 1983)
[c] Numerical Coulomb-like approximation (Lindgård et al., 1980)
[d] Relativistic Hartree–Fock calculation with account for core polarisation effects (Migdałek and Baylis, 1978)
[e] Relativistic Hartree–Fock calculation with model potential accounting for exchange and core polarisation (Migdałek, 1978)
[f] Relativistic Hartree–Fock calculation with model potential and core polarisation (Migdałek and Baylis, 1979)
[g] Calculation using the level-crossing measurement of lifetimes and configuration coupling coefficient deduced by fitting other experimental measurements of lifetimes and relative oscillator strengths (Siefart et al., 1974)
[h] Atomic absorption measurements on flames (Lvov, 1970)
[i] Atomic-beam absorption (Bell and Tubbs, 1970)
[j] Critical survey of experimentally-determined oscillator strengths (Corliss, 1970)
[k] Curves of growth in absorption measurement (Moise, 1966)
[l] Rozhdestvenskii's hook method (Slavenas, 1966)
[m] Atomic-beam absorption (Bell et al., 1958)
[n] Arc emission measurements (Allen and Asaad, 1957)

Table 2. FMP-calculated transition dipole moments (oscillator strengths f_{ik}, transition probabilities A_{ki}) between the Cu I states observed in the present work. The energies of all levels are taken from the present measurement except those for 4f and 7s levels taken from Shenstone (1948). The air wavelengths λ are calculated using these energy values.

Transition	Lower level (cm^{-1})	Upper level (cm^{-1})	ν (cm^{-1})	λ (nm)	f_{ik}	A_{ki} (s^{-1})
$5f_{\frac{7}{2}}$–$6g_{\frac{9}{2}}$	57911.09	59266.676	1355.586	7374.87	1.14	1.12×10^6
$5f_{\frac{5}{2}}$–$6g_{\frac{7}{2}}$	57905.041	59267.202	1362.161	7339.28	1.17	1.08×10^6
$5f_{\frac{7}{2}}$–$6g_{\frac{7}{2}}$	57911.09	59267.202	1356.112	7372.01	3.26×10^{-2}	3.99×10^4
$6p_{\frac{3}{2}}$–$7s_{\frac{1}{2}}$	54784.081	56671.387	1887.306	5297.11	4.26×10^{-1}	2.02×10^6
					3.606×10^{-1} [a]	1.714×10^6 [a]
$6s_{\frac{1}{2}}$–$6p_{\frac{3}{2}}$	52848.752	54784.081	1935.329	5165.67	1.02	1.28×10^6
					1.126×10^{-1} [a]	1.406×10^6 [a]
$5f_{\frac{7}{2}}$–$7g_{\frac{9}{2}}$	57911.09	60074.98	2163.890	4620.05	2.23×10^{-1}	5.58×10^5
$5f_{\frac{7}{2}}$–$7g_{\frac{7}{2}}$	57911.09	60076.159	2165.069	4617.53	6.40×10^{-3}	2.00×10^4
$5f_{\frac{5}{2}}$–$7g_{\frac{7}{2}}$	57905.041	60076.159	2171.118	4604.67	2.31×10^{-1}	5.46×10^5
$6d_{\frac{5}{2}}$–$7f_{\frac{7}{2}}$	57895.084	60071.51	2176.426	4593.44	1.86×10^{-1}	4.41×10^5
$6s_{\frac{1}{2}}$–$6p_{\frac{1}{2}}$	52848.752	55027.763	2179.011	4587.99	5.34×10^{-1}	1.69×10^6
$4f_{\frac{5}{2}}$–$5g_{\frac{7}{2}}$	55429.8	57924.61	2494.810	4007.23	1.34	4.19×10^6
$4f_{\frac{7}{2}}$–$5g_{\frac{9}{2}}$	55426.3	57924.075	2497.775	4002.47	1.31	4.35×10^6
$4f_{\frac{7}{2}}$–$5g_{\frac{7}{2}}$	55426.3	57924.61	2498.310	4001.61	3.73×10^{-2}	1.55×10^5
$5d_{\frac{5}{2}}$–$5f_{\frac{5}{2}}$	55390.569	57905.041	2514.472	3975.89	4.16×10^{-2}	1.76×10^5
					4.140×10^{-2} [a]	1.745×10^5 [a]
$5d_{\frac{3}{2}}$–$5f_{\frac{5}{2}}$	55387.621	57905.041	2517.420	3971.24	8.73×10^{-1}	2.46×10^6
					8.667×10^{-1} [a]	2.443×10^6 [a]
$5d_{\frac{5}{2}}$–$5f_{\frac{7}{2}}$	55390.569	57911.09	2520.521	3966.35	8.28×10^{-1}	2.63×10^6
					8.235×10^{-1} [a]	2.611×10^6 [a]
$6p_{\frac{1}{2}}$–$6d_{\frac{3}{2}}$	55027.763	57893.028	2865.265	3489.13	3.80×10^{-1}	1.04×10^6
					3.532×10^{-1} [a]	9.672×10^5 [a]
$6p_{\frac{3}{2}}$–$6d_{\frac{3}{2}}$	54784.081	57893.028	3108.947	3215.65	2.59×10^{-2}	1.67×10^5
					2.247×10^{-2} [a]	1.448×10^5 [a]
$5p_{\frac{1}{2}}$–$6s_{\frac{1}{2}}$	49383.263	52848.752	3465.489	2884.81	3.27×10^{-1}	2.62×10^6
					2.871×10^{-1} [a]	2.299×10^6 [a]
$5p_{\frac{3}{2}}$–$6s_{\frac{1}{2}}$	49382.949	52848.752	3465.803	2884.55	3.27×10^{-1}	5.25×10^6
					2.870×10^{-1} [a]	4.599×10^6 [a]
$4f_{\frac{5}{2}}$–$6g_{\frac{7}{2}}$	55429.8	59267.202	3837.402	2605.22	1.85×10^{-1}	1.37×10^6
$4f_{\frac{7}{2}}$–$6g_{\frac{9}{2}}$	55426.3	59266.676	3840.376	2603.20	1.80×10^{-1}	1.42×10^6
$4f_{\frac{7}{2}}$–$6g_{\frac{7}{2}}$	55426.3	59267.202	3840.902	2602.84	5.16×10^{-3}	5.08×10^4
$4f_{\frac{5}{2}}$–$7g_{\frac{7}{2}}$	55429.8	60076.159	4646.359	2151.64	5.96×10^{-2}	6.43×10^5
$4f_{\frac{7}{2}}$–$7g_{\frac{9}{2}}$	55426.3	60074.98	4648.68	2150.56	5.77×10^{-2}	6.66×10^5
$4f_{\frac{7}{2}}$–$7g_{\frac{7}{2}}$	55426.3	60076.159	4649.859	2150.02	1.66×10^{-3}	2.40×10^4

[a] Numerical Coulomb-like approximation (Lindgård et al., 1980)

Table 3. Experimental Cu I lines and their identification. The decay time, T, was calculated by exponential fitting of the measured time profiles of the corresponding lines.

Wavenumber (cm^{-1})	Intensity (arb. units)	SNR	FWHM (cm^{-1})	Decay time (μs)	Identification
1887.307(6)	1.30×10^4	17	0.083(16)	12.1(44)^b	$6p_{\frac{3}{2}}$–$7s_{\frac{1}{2}}$
1935.313(2)	6.58×10^4	63	0.106(5)	5.88(221)^b	$6s_{\frac{1}{2}}$–$6p_{\frac{3}{2}}$
2163.890(16)	3.42×10^2	6.2	0.104(46)	16.2(41)^a	$5f_{\frac{7}{2}}$–$7g_{\frac{9}{2}}$
2171.118(18)	1.64×10^2	4.6	0.074(55)	9.50(266)^a	$5f_{\frac{5}{2}}$–$7g_{\frac{7}{2}}$
2176.426(16)	2.16×10^2	5.6	0.077(43)	12.8(34)^b	$6d_{\frac{5}{2}}$–$7f_{\frac{7}{2}}$
2179.011(3)	7.68×10^4	58	0.065(10)	9.06(479)^a	$6s_{\frac{1}{2}}$–$6p_{\frac{1}{2}}$
2494.8098(3)	2.98×10^5	63	0.038(1)	11.7(42)^b	$4f_{\frac{5}{2}}$–$5g_{\frac{7}{2}}$
2497.7750(3)	3.77×10^5	121	0.041(1)	11.3(36)^b	$4f_{\frac{7}{2}}$–$5g_{\frac{9}{2}}$
2513.814(4)	4.65×10^3	8.4	0.048(13)	11.5(41)^b	$5d_{\frac{5}{2}}$–$5f_{\frac{5}{2}}$
2517.4511(3)	1.03×10^5	78	0.051(1)	15.0(57)^b	$5d_{\frac{3}{2}}$–$5f_{\frac{5}{2}}$
2521.0550(3)	1.58×10^5	129	0.049(1)	14.9(57)^b	$5d_{\frac{5}{2}}$–$5f_{\frac{7}{2}}$
2865.233(2)	2.32×10^4	37	0.062(5)	7.93(167)^b	$6p_{\frac{1}{2}}$–$6d_{\frac{3}{2}}$
3110.955(4)	2.06×10^4	27	0.087(11)	8.53(214)^b	$6p_{\frac{3}{2}}$–$6d_{\frac{5}{2}}$
3465.481(4)	8.46×10^4	10	0.089(13)	5.06(87)^b	$5p_{\frac{1}{2}}$–$6s_{\frac{1}{2}}$
3465.8044(7)	1.70×10^5	23	0.048(2)	5.25(90)^b	$5p_{\frac{3}{2}}$–$6s_{\frac{1}{2}}$
3837.402(12)	7.49×10^3	9.5	0.193(36)	8.51(209)^a	$4f_{\frac{5}{2}}$–$6g_{\frac{7}{2}}$
3840.376(15)	9.64×10^3	11	0.235(47)	14.7(190)^a	$4f_{\frac{7}{2}}$–$6g_{\frac{9}{2}}$

^{a}Time profile demonstrates significant deviation from the exponential decay

^{b}The decay curve has essentially non-exponential form with a plateau or secondary maxima; τ value is absent or roughly approximate

several lines display essentially non-exponential behavior including some "plateaux" or even secondary maxima at 35–50 μs after the laser shot. Their decay time, T, values are therefore estimated in Table 3 in a rough approximation; it is seen from this table that for essentially non-exponential decays the uncertainity ΔT is of the same order of magnitude as T itself. Note that this temporal decay is due to a complex combination of the collisional cascade repopulation of the emitting levels (Civiš et al., 2010) and the transfer processes in ablation products (Kawaguchi et al., 2008). The decay times T given in Table 3 is not related to the radiative lifetimes of Cu $3d^{10}\,nl$ levels which are at least two orders shorter (typical orders are $\sim 10^1$–10^3 ns (Fu et al., 1995)).

After the assignment we refined the energy values for some levels involved with the classified transitions; the revised values of these energies are presented in Table 4. This procedure was similar to that used in the previous paper (Civiš et al., 2010), but unfortunately there is no high precision data on these levels, so the overall uncertainty of the refined level energy values is roughly that achieved in the old measurements (0.01–0.03 cm^{-1} by Shenstone (1948) and 0.07 cm^{-1} by Longmire et al. (1980)). Nevertheless, the difference between the energy value obtained in this work for $5f_{\frac{7}{2}}$ level and that reported long ago (Shenstone, 1948) is about 2.5 cm^{-1}and lies beyond

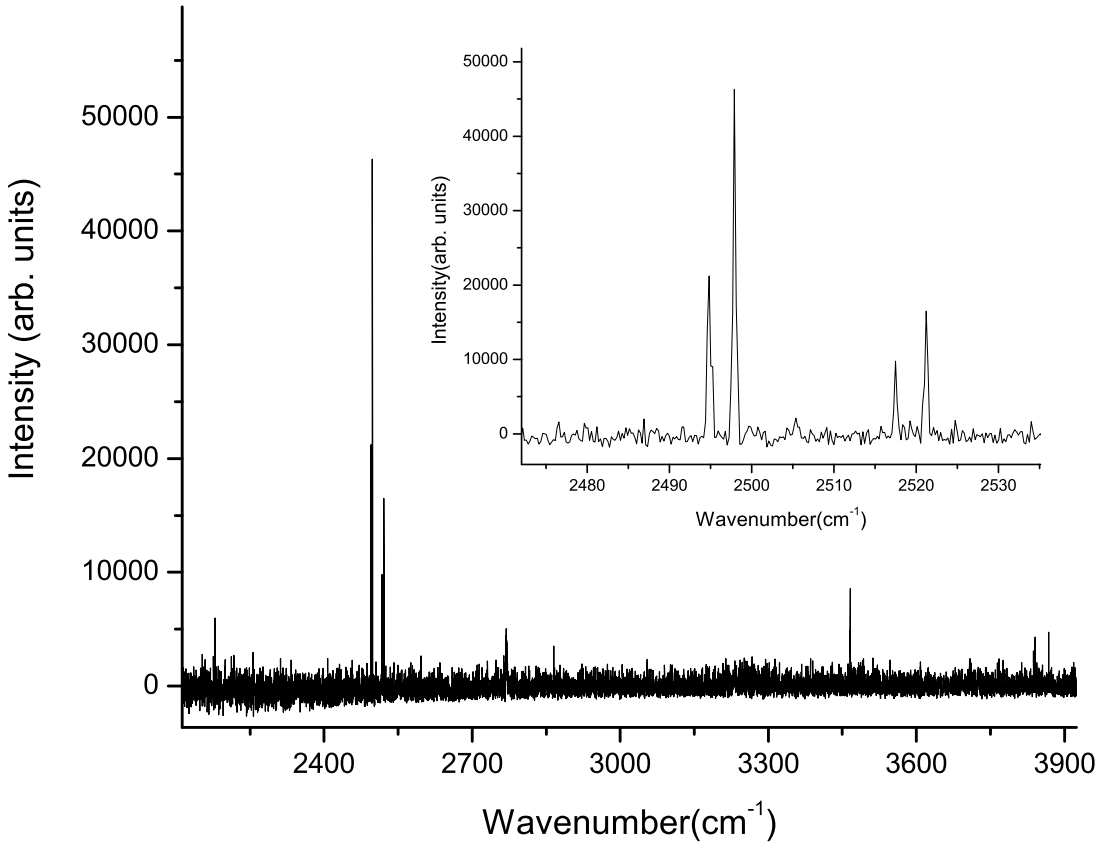

Figure 1. Observed emission IR spectrum of Cu I with a detailed structure of the most prominent lines around 2480–2530 cm^{-1}. Both the inset and the main spectrum correspond to the resolution of 0.017 cm^{-1}.

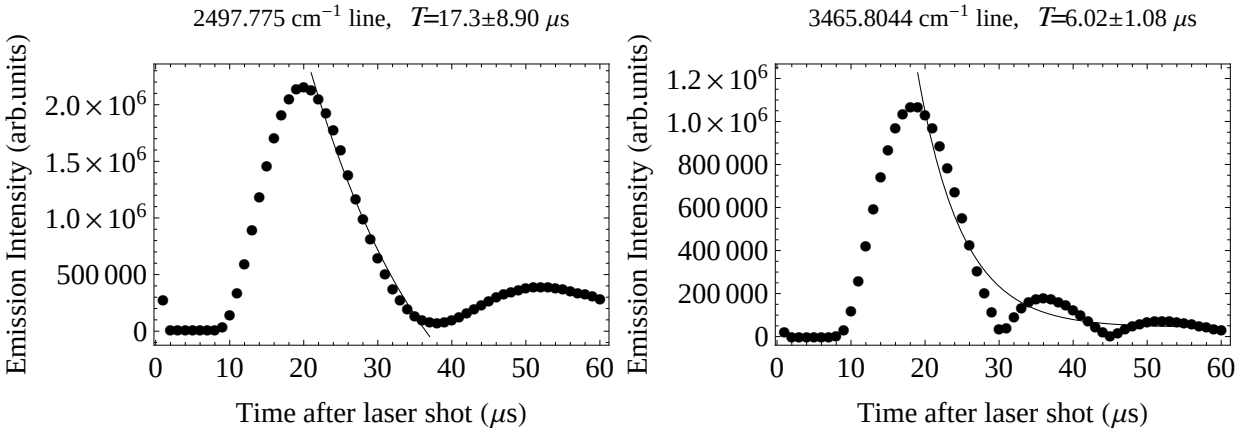

Figure 2. The time profiles of some observed Cu I lines (dots) and their fit with exponential decay (solid curves)

the uncertainty limits. Due to the better resolution of our measurements, the values listed in the Table 4 can be considered to be more accurate.

It is interesting to note that the fine-structure 5p doublet (fine-structure splitting is about 0.3 cm^{-1}) is well resolved in our experiment, unlike the previous measurements (Shenstone, 1948; Longmire et al., 1980) where only a single blended line was observed. The ratio of the $5p_{\frac{3}{2}}$–$6s_{\frac{1}{2}}$ and $5p_{\frac{1}{2}}$–$6s_{\frac{1}{2}}$ transition intensities is close to the theoretical nonrelativistic value 2:1. This doublet is shown in Figure 3 in different resolutions, the $5p_{\frac{1}{2}}$–$6s_{\frac{1}{2}}$ component demonstrates hyperfine splitting.

4. Conclusion

This work continues the series of studies of emission IR spectra of metal vapors formed in ablation by a pulsed laser radiation (Civiš et al., 2010; Civiš et al., 2010) where TR FTIR spectroscopy is applied to observations of the emission arising after the irradiation of a copper target with a pulsed laser. The knowledge of Cu spectra is extended by reporting 18 lines not previously observed. All are classified as due to transitions between low-excited states: $3d^{10}\,ns$ with $n = 6, 7$, $3d^{10}\,np$ ($n = 5, 6$), $3d^{10}\,nd$ ($n = 5, 6$), $3d^{10}\,nf$ ($n = 4, 5, 7$) and $3d^{10}\,ng$ ($n = 5, 6, 7$).

The line classification is performed using relative line strengths expressed in terms of transition dipole matrix elements calculated with the help of the Fues model potential; these calculations show agreement with the experimental and calculated data available in the literature. In addition to these data we calculate the transition probabilities and oscillator strengths for transitions between the reported $3d^{10}\,nl_j$ states of Cu I.

This study reports revised values for energies of eleven known and of seven previously not reported $3d^{10}\,nl$ levels of neutral Cu with n = 4–7 and l = 5–7. The newly-found 5g, 6g and 7g ^{2}G terms are inverted. We also record time profiles of the observed lines as functions of the delay time (0–60 μs) after the laser shot with maxima of emission intensity at 18–20 μs after the shot. Some lines display single-exponential temporal decay, while the decay of other lines is essentially non-exponential and demonstrates some "plateaux" (or even secondary maxima) at 40–50 μs after the laser shot. The approximate decay time for different lines varies in the 5–15 μs range.

Acknowledgments

This work was financially supported by the Grant Agency of the Academy of Sciences of the Czech Republic (Grants No. IAA400400705 and KAN 100500652).

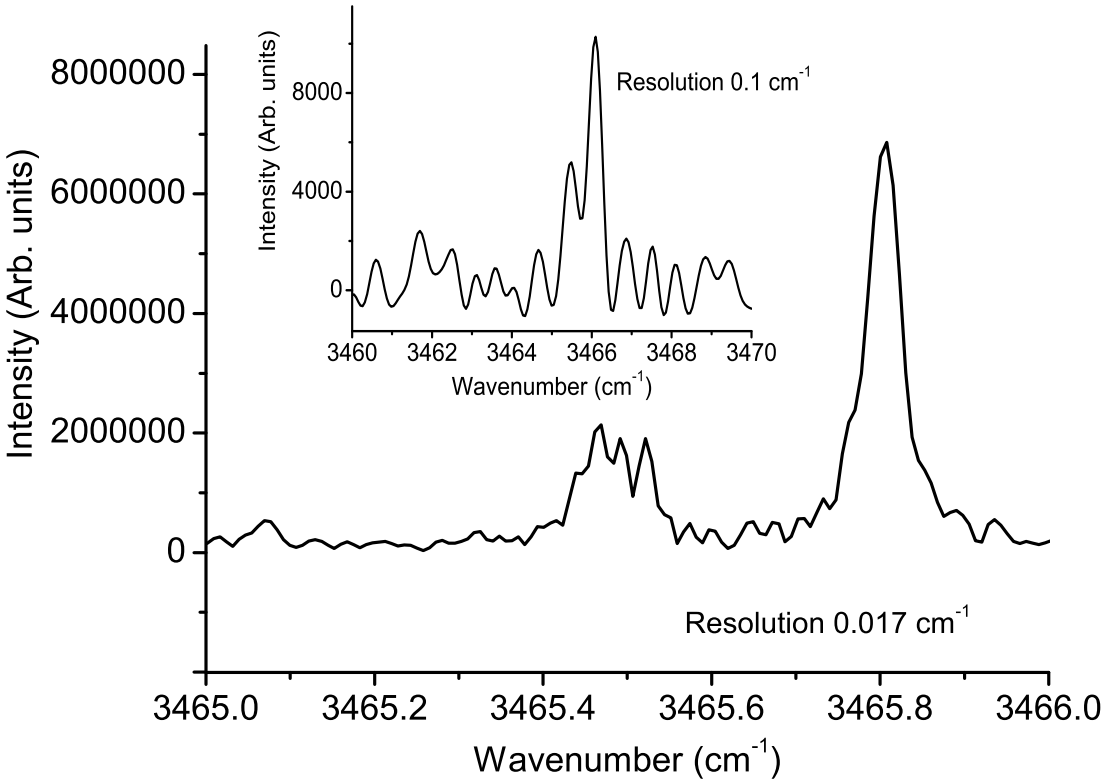

Figure 3. The $5p_{\frac{1}{2},\frac{3}{2}}$–$6s_{\frac{1}{2}}$ doublet lines of Cu I in two different resolutions. The $5p_{\frac{1}{2}}$–$6s_{\frac{1}{2}}$ component (with center of gravity at 3465.481 cm^{-1}) is split due to hyperfine structure.

Table 4. Revised values of some levels of Cu I

Term	Energy (cm^{-1})	Other sources
$3d^{10}\,5p_{\frac{1}{2}}$	49383.263(23)	49383.26[a]
$3d^{10}\,5p_{\frac{3}{2}}$	49382.949(14)	49382.95[a]
$3d^{10}\,5d_{\frac{3}{2}}$	55387.621(11)	55387.668[a]
$3d^{10}\,5d_{\frac{5}{2}}$	55390.569(9)	55391.292[a]
$3d^{10}\,5f_{\frac{5}{2}}$	57905.041(14)	57905.2[a], 57905.23[b]
$3d^{10}\,5f_{\frac{7}{2}}$	57911.090(12)	57908.7[a]
$3d^{10}\,5g_{\frac{7}{2}}$	57924.610(30)	This work
$3d^{10}\,5g_{\frac{9}{2}}$	57924.075(30)	This work
$3d^{10}\,6s_{\frac{1}{2}}$	52848.752(9)	52848.749[a]
$3d^{10}\,6p_{\frac{1}{2}}$	55027.763(26)	55027.74[a], 55027.713[b]
$3d^{10}\,6p_{\frac{3}{2}}$	54784.081(21)	54784.06[a], 54784.073[b]
$3d^{10}\,6d_{\frac{3}{2}}$	57893.028(24)	57893.05[a]
$3d^{10}\,6d_{\frac{5}{2}}$	57895.084(24)	57895.1[a]
$3d^{10}\,6g_{\frac{7}{2}}$	59267.202(33)	This work
$3d^{10}\,6g_{\frac{9}{2}}$	59266.676(34)	This work
$3d^{10}\,7f_{\frac{7}{2}}$	60071.510(30)	This work
$3d^{10}\,7g_{\frac{7}{2}}$	60076.159(23)	This work
$3d^{10}\,7g_{\frac{9}{2}}$	60074.980(20)	This work

[a] Shenstone (1948)
[b] Longmire et al. (1980)

References

Allen C W and Asaad A S 1957 *Mon. Not. R. Astron. Soc.* **117**(1), 36–49.

Baig M A, Hanif M, Bhatti S A and Hormes J 1997 *J. Phys. B* **30**(23), 5381–5399.
URL: *http://stacks.iop.org/0953-4075/30/i=23/a=007*

Baig M A, Rashid A, Hanif M, Dussa W, Ahmad I and Hormes J 1992 *Phys. Rev. A* **45**(3), 2108–2111.

Bell G D, Davis M H, King R B and Routly P M 1958 *Astrophys. J.* **127**, 775–796.

Bell G D and Tubbs E F 1970 *Astrophys. J.* **159**, 1093–1100.

Biémont E 1994 *in* D. M. Rabin, J. T. Jefferies, & C. Lindsey, ed., 'Infrared Solar Physics' Vol. 154 of *IAU Symposia* Int. Astron. Union Kluwer Academic Publ. PO Box 17, 3300 AA Dordrecht, Netherlands pp. 501–510. 154th Symposium of the International-Astronomical-Union - 1st International Meeting devoted to Infrared Physics, Tucson, AZ, Mar. 02–06, 1992.

Bihain G, Israelian G, Rebolo R, Bonifaci P and Molaro P 2004 *Astron. Astrophys.* **423**(3), 777–786.

Carlsson J 1988 *Phys. Rev. A* **38**(4), 1702–1710.

Civiš S, Matulková I, Cihelka J, Kawaguchi K, Chernov V E and Buslov E Y 2010 *Phys. Rev. A* **81**(1), 012510.

Civiš S, Matulková I, Cihelka J, Kubelík P, Kawaguchi K and Chernov V E 2010 *Phys. Rev. A* **82**(2), 022502.

Corliss C H 1970 *J. Res. Nat. Bur. Stand.* **A 74**, 781–790.

Cowan J J, Sneden C, Burles S, Ivans I I, Beers T C, Truran J W, Lawler J E, Primas F, Fuller G M, Pfeiffer B and Kratz K 2002 *Astrophys. J.* **572**, 861–879.

Cunha K, Smith V V, Suntzeff N B, Norris J E, Da Costa G S and Plez B 2002 *Astron. J.* **124**(1), 379–388.
URL: *http://stacks.iop.org/1538-3881/124/i=1/a=379*

Curtis L J and Theodosiou C E 1989 *Phys. Rev. A* **39**(2), 605–615.

Ecuvillon A, Israelian G, Santos N C, Mayor M, Villar V and Bihain G 2004 *Astron. Astrophys.* **426**(2), 619–630.

Fu K, Jogwich M, Knebel M and Wiesemann K 1995 *At. Data Nucl. Data Tables* **61**(1), 1–30.

Furusawa H, Sakka T and Ogata Y H 2004 *J. Appl. Phys.* **96**(2), 975–982.
URL: *http://link.aip.org/link/?JAP/96/975/1*

Grevesse N and Noels A 1994 *Phys. Scr.* **T51**, 47–50. 25th Conference of the European-Group-for-Atomic-Spectroscopy (EGAS), Caen, France, Jul. 13–16, 1993.

Hannaford P and Lowe R M 1983 *Opt. Eng.* **22**(5), 532–544.

Honda S, Aoki W, Ishimaru Y and Wanajo S 2007 *Astrophys. J.* **666**(2, Part 1), 1189–1197.
URL: *http://iopscience.iop.org/0004-637X/666/2/1189*

Johansson S 2005 *in* Kaufl, H. U. and Siebenmorgen, R. and Moorwood, A., ed., 'High Resolution Infrared Spectroscopy In Astronomy, Proceedings' ESO Astrophysics Symposia ESO Springer–Verlag Berlin Heidelberger Platz 3, D-14197 Berlin, Germany pp. 62–67. ESO Workshop on High Resolution Infrared Spectroscopy in Astronomy, Garching, Germany, Nov. 18–21, 2003.
URL: *http://www.springerlink.com/content/yg313t42u72643j6/*

Jones H R A, Viti S, Tennyson J, Barber B, Harris G, Pickering J C, Blackwell-Whitehead R, Champion J P, Allard F, Hauschildt P H, Jorgensen U G, Ehrenfreund P, Stachowska E, Ludwig H G, Martin E L, Pavlenko Y, Lyubchik Y and Kurucz R L 2005 *Astron. Nachr.* **326**(10), 920–924. Ultralow-Mass Star Formation and Evolution Workshop, La Palma, SPAIN, JUN 28-JUL 01, 2005.

Jorissen A 2004 *Phys. Scr.* **T112**, 73–86.

Kawaguchi K, Sanechika N, Nishimura Y, Fujimori R, Oka T N, Hirahara Y, Jaman A and Civiš S 2008 *Chem. Phys. Lett.* **463**(1–3), 38–41.

Kerber F, Nave G, Sansonetti C J and Bristow P 2009 *Phys. Scr.* **T134**, 014007.

Lindgård A, Curtis L J, Martinson I and Nielsen S E 1980 *Phys. Scr.* **21**, 47–62.

Longmire M S, Brown C M and Ginter M L 1980 *J. Opt. Soc. Am.* **70**(4), 423–429.

Lvov B V 1970 *Opt. Spectrosk.* **28**(1), 8–12.

MacAdam K B, Dyubko S F, Efremov V A, Gerasimov V G and Kutsenko A S 2009 *J. Phys. B* **42**, 165009.

Martin W C and Sugar J 1969 *J. Opt. Soc. Am.* **59**(10), 1266–1280.

Matteucci F, Raiteri C M, Busson M, Gallino R and Gratton R 1993 *Astron. Astrophys.* **272**(2), 421–429.

Migdałek J 1978 *J. Quant. Spectrosc. Radiat. Transfer* **20**(1), 81–87.

Migdałek J and Baylis W E 1978 *J. Phys. B* **11**(17), L497–L501.

Migdałek J and Baylis W E 1979 *J. Phys. B* **12**(7), 1113.
URL: *http://stacks.iop.org/0022-3700/12/i=7/a=014*

Mishenina T V, Kovtyukh V V, Soubiran C, Travaglio C and Busso M 2002 *Astron. Astrophys.* **396**(1), 189–201.

Moise N L 1966 *Astrophys. J.* **144**(2), 774–781.

Nilsson H 2009 *Phys. Scr.* **T134**, 014009. 9th International Conference on Atomic Spectroscopy and Oscillator Strengths for Astrophysical and Laboratory Plasma, Lund, Sweden, Aug. 07–10, 2007.
URL: *http://iopscience.iop.org/1402-4896/2009/T134/014009*

Pickering J C 1999 *Phys. Scr.* **T83**, 27–34. 6th International Colloquium on Atomic Spect and Oscillator Strengths (ASOS 6), Victoria, Canada, Aug. 09–13, 1998.

Prochaska J X, Naumov S O, Carney B W, McWilliam A and Wolfe A M 2000 *Astron. J.* **120**(5), 2513–2549.

Rossa M, Rinaldi C A and Ferrero J C 2009 *J. Appl. Phys.* **105**(6), 063306.
URL: *http://ieeexplore.ieee.org/xpl/ freeabs$_a$ll.jsp?arnumber* = 5133154

Ryde N 2009 *Phys. Scr.* **T134**, 014001. 9th International Conference on Atomic Spectroscopy and Oscillator Strengths for Astrophysical and Laboratory Plasma, Lund, Sweden, Aug. 07–10, 2007.
URL: *http://iopscience.iop.org/1402-4896/2009/T134/014001*

Ryde N 2010 *Astron. Nachr.* **331**(4), 433–448.

Shenstone A G 1948 *Philos. Trans. R. Soc. London, Ser. A* **241**(832), 297–322.

Siefart E, Ney J, Bucka H and Bolouri H 1974 *J. Phys. B* **7**(11), 1279–1283.
URL: *http://stacks.iop.org/0022-3700/7/i=11/a=014*

Simmerer J, Sneden C, Ivans I I, Kraft R P, Shetrone M D and Smith V V 2003 *Astron. J.* **125**(4), 2018–2028.
URL: *http://stacks.iop.org/1538-3881/125/i=4/a=2018*

Slavenas I Y Y 1966 *Opt. Spectrosk.* **20**(3), 485–487.

Sneden C, Gratton R G and Crocker D A 1991 *Astron. Astrophys.* **246**(2), 354–367.

Sobeck J S, Primas F, Sneden C and Ivans I I 2008 *in* B. W O'Shea, A Heger and T Abel, eds, 'First Stars III' Vol. 990 of *AIP Conference Proceedings* Los Alamos Natl Lab; New Mexico Consortium Inst Adv Study; Kavli Inst Particle Astrophys & Cosmol; Joint Inst Nucl Astrophys Amer. Inst. Physics 2 Huntington Quadrangle, STE 1NO1, Melville, NY 11747-4501 USA pp. 187–191. International Conference on First Stars III, Santa Fe, NM, JUL 15-20, 2007.
URL: *http://link.aip.org/link/?APC/990/187/1*

Tondello G 1973 *J. Opt. Soc. Am.* **63**(3), 346–352.

Wahlgren G M, Carpenter K G and Norris R P 2009 *in* E Stempels, ed., 'Cool Stars, Stellar Systems and the Sun' Vol. 1094 of *AIP Conference Proceedings* Royal Astron Soc; Scottish Univ Phys Alliance; European Space Agcy; NASA Astrobiol Inst Amer. Inst. Physics 2 Huntington Quadrangle, STE 1NO1, Melville, NY 11747-4501 USA pp. 892–895. 15-th Cambridge Workshop on Cool Stars, Stellar Systems and the Sun, St. Andrews, Scotland, Jul. 21–25, 2008.
URL: *http://link.aip.org/link/?APC/1094/892/1*